

Fourth-order partial-coherence effects in the formation of integrated-intensity gratings with pulsed light sources

Rick Trebino, Eric K. Gustafson, and A. E. Siegman

Edward L. Ginzton Laboratory, Stanford University, Stanford, California 94305

Received December 20, 1985; accepted May 5, 1986

We performed theoretical calculations of the relative diffraction efficiency of partially coherent light-induced integrated-intensity gratings using pulsed sources, paying particular attention to thermal gratings. We provided a simple intuitive picture of the phenomenon and then calculated exact expressions that, unlike instantaneous-intensity-grating results, necessarily require the use of fourth-order coherence functions. Assuming several radiation models, we evaluated these expressions and found that the results proved to be insensitive to the specific radiation model assumed. The application of these results to a previously performed pulsed-laser experiment yielded a better fit to the data than an expression involving only second-order coherence, which is valid only in the cw limit. We included the effects of grating decay and, in addition, compared the use of integrated-intensity gratings for ultrashort-pulse-length measurement with standard techniques. Finally, we calculated expressions for the relative diffraction efficiency of integrated-intensity gratings created with excitation beams from two separate and independent sources of different frequency, and we report an experiment whose results were found to agree with this theory.

1. INTRODUCTION

Integrated-intensity gratings, induced in a material by interfering light beams, arise in many nonlinear-optical experimental techniques. In some degenerate four-wave mixing materials, diffraction from integrated-intensity gratings yields efficient phase-conjugate reflection.^{1,2} In short-pulse transient-grating experiments, the creation of integrated-intensity gratings permits the measurement of diffusivity constants and also the study of acoustic waves created in the process.³⁻⁵ In addition, the large magnitude of some integrated-intensity-grating effects has led to their use in schemes for the measurement of ultrashort pulse lengths⁶ and coherence times.^{7,8} On the negative side, integrated-intensity gratings in the form of thermal gratings often prove to be a nuisance in laser techniques intended to measure population, but not thermal, effects.⁹ And in short-pulse excite-probe experiments, the "coherence spike" often originates from a thermal grating or other integrated-intensity grating.¹⁰

In all light-induced-grating interactions, the partial-coherence properties of the excitation beams play an important role. We have known from the time of Michelson that the ability to form integrated-intensity fringes requires good temporal coherence between the excitation beams.¹¹ A single light source, providing both beams with a relative delay of less than each beam's coherence time, is generally required for intensity fringes to be obtained. The use of a large delay generally results in weak fringes, and worse, two separate sources produce no fringes at all.

When integrated-intensity fringes arise in *pulsed-laser*, induced-grating experiments, however, the situation is somewhat different from the well-known example mentioned above. First, rather than using radiation of infinite duration, these experiments employ a series of pulses, each pulse being a finite number of coherence times in length. Second, rather than the actual fringes, what is observed is a

beam diffracted by the fringes. And by measuring only the *intensity* of the diffracted beam, we lose the information on its *phase*, which consequently deprives us of information on the induced-grating phase.

Why are these differences important? The loss of phase information is important because, by measuring only the amplitude of the grating fringes, we measure an inherently positive quantity. And by using excitation pulses a finite number of coherence times in duration, the total washout of the intensity fringes that can take place in cw experiments does not occur. On each pulse, then, we measure an inherently positive diffraction efficiency. That positive quantity is then averaged over many pulses to yield a potentially significant signal. Thus pulsed-laser, integrated-intensity-grating experiments can yield large diffraction efficiencies, while cw experiments, or those that are sensitive to the instantaneous phase of the fringes, will measure very little fringe strength.

In this paper we give an intuitive picture of integrated-intensity-grating formation with partially coherent light pulses. We derive theoretical expressions for the diffraction efficiencies of integrated-intensity gratings, and we show that these expressions necessarily involve fourth-order coherence functions. This mathematical theory differs from the second-order coherence-function theory of the Michelson interferometer and related fringe-producing devices¹¹ because induced-grating experiments measure the *squared* amplitude of the fringes: the diffracted radiation *field* is proportional to the complex grating amplitude, and the diffracted *intensity* is what is measured. Because the complex grating amplitude is proportional to the product of the two excitation-beam envelopes, the product of *four* radiation fields will occur in any expression for the observed diffracted intensity. Any theoretical treatment of induced gratings using partially coherent light pulses will then necessarily involve *fourth-order* coherence functions.

This fourth-order theory reduces in the cw limit to the

well-known second-order theory; the deviations from the second-order theory will be proportional to the ratio of the coherence time, τ_c , to the pulse length, τ_p , of the excitation radiation. Only in the past few years have light sources achieved Fourier-transform-limited quality, for which $\tau_c/\tau_p \sim 1$, so that the above deviations from the second-order theory have only recently become observable. And, in fact, several recently performed pulsed experiments exhibit deviations from the second-order theory. A variable-delay, integrated-intensity-grating experiment performed by Eichler *et al.*⁷ exhibited greater diffraction for large delays than were predicted by the second-order theory. In addition, various thermal-grating experiments employing excitation beams from two separate lasers—for which the second-order theory predicts no diffraction at all—observe such strong diffraction that other (instantaneous-intensity) effects have been obscured.^{9,12} The fourth-order theory developed here-in will accurately explain these experiments.

We will consider the special case of *thermal* gratings because typical thermal-grating decay times are generally quite long compared with Q-switched- and mode-locked-laser pulses, so that thermal gratings induced by such pulses are in general modeled accurately as integrated-intensity gratings. Other types of induced gratings will also behave as integrated-intensity gratings, and the quantities used here can be relabeled easily to describe them.

We derive exact expressions for the relative magnitude of the (integrated-intensity) thermal-grating diffraction efficiency for several radiation models, specifically, amplitude-stabilized and thermal radiation with Lorentzian and Gaussian line shapes. For thermal radiation, these expressions reduce to particularly useful and intuitive results when the radiation coherence time is much less than the pulse length. In this regime, our expressions contain two terms, one equal to the squared magnitude of the second-order coherence function and the other proportional to the pulse envelope autocorrelation function. Applying these results to a previously performed experiment,⁷ we obtain a better fit than that obtained with previous theories.

In addition, we discuss the merits of thermal-grating techniques for the measurement of laser pulse lengths and coherence times and compare these techniques with standard methods. Finally, we calculate the relative diffraction efficiency of an integrated-intensity grating using two independent excitation sources, and we report an experiment whose results agree with the predictions of this theory.

Previous theoretical work on thermal and other integrated-intensity gratings induced with pulsed partially coherent radiation include that of Vardeny and Tauc,¹⁰ who obtain some of the general expressions contained here but do not consider specific radiation models. Eichler *et al.*⁷ do consider specific models for the input radiation but employ a second-order theory, obtaining only coherence effects and not pulse-length effects. Idiutulin and Teryaev,⁶ on the other hand, obtain the pulse autocorrelation term but not the coherence term. Many authors have treated the so-called “coherent-coupling spike” of ultrashort-pulse, excite-probe experiments¹³⁻¹⁶ and some have included integrated-intensity effects and fourth-order effects, but none have considered specific radiation models. Grossman and Shemwell¹⁷ calculated the effects of poor coherence on phase conjugation by degenerate four-wave mixing. Finally, fourth- and

higher-order coherence functions arise in a number of phenomena; numerous calculations involving them exist in the literature.^{11,18,19}

2. PRELIMINARY THEORY: AN INTUITIVE PICTURE AND A REVIEW OF INTEGRATED-INTENSITY-GRATING THEORY

A simple argument shows how, despite poor coherence between excitation beams, a pulsed-laser-induced, integrated-intensity grating will diffract light and, in addition, approximately how much light will be diffracted. Suppose the excitation pulses are N coherence times long. The phase of the intensity-fringe pattern will change randomly (and, we assume for simplicity, discretely) on the scale of a coherence time. After N coherence times, the integrated-intensity-grating complex amplitude, A , will be the *sum* of the individually contributed gratings from each coherence-time period:

$$A = \sum_{m=1}^N \exp(i\phi_m), \quad (1)$$

where ϕ_m is the phase of the fringe pattern during the m th period. The expected diffraction efficiency, $\langle \eta \rangle$, is proportional to the ensemble expectation of $|A|^2$ and will be

$$\langle \eta \rangle \propto \left\langle \left| \sum_{m=1}^N \exp(i\phi_m) \right|^2 \right\rangle. \quad (2)$$

For randomly distributed individual phases, ϕ_m , the expectation value takes on the value N . Thus, the diffraction efficiency will not be zero. For comparison, suppose that the coherence between the beams is perfect. Then, throughout the pulse (continue to break the pulse down into N increments), all contributions to the grating will be in phase, i.e., all ϕ_m are equal. As a result, in this case, $\langle \eta \rangle \propto N^2$. Comparing the diffraction efficiencies of these two cases indicates that poor coherence results in a lessened diffraction efficiency by a factor of N , the ratio of the pulse length to the coherence time. In the cw limit, $N \rightarrow \infty$, and this reduction is infinite, but in pulsed-laser experiments N will be a finite number and a considerable diffraction efficiency will remain.²⁰

This argument shows that when the excitation sources of an integrated-intensity grating are independent, the diffraction efficiency of the grating will be reduced by a factor of the order of τ_c/τ_p , where τ_c is the coherence time and τ_p is the pulse length. The argument applies to experiments employing one light source in which the relative delay between the two excitation beams derived from this source is much greater than the source coherence time. It also applies to experiments employing two independent light sources of the same frequency. Thus, despite the minimal coherence between the two excitation beams in these two types of experiment, a finite diffraction efficiency will exist.

To formalize the above argument and to allow for specific radiation models, we must take into account the actual time dependences of the excitation fields. Consequently, we consider two quasi-monochromatic plane waves of the same frequency (ω) and polarization (\hat{e})

$$\mathcal{E}_1(\mathbf{r}, t) = \text{Re } E_1(t) \exp i(\omega t - \mathbf{k}_1 \cdot \mathbf{r}) \hat{e},$$

$$\mathcal{E}_2(\mathbf{r}, t) = \text{Re } E_2(t) \exp i(\omega t - \mathbf{k}_2 \cdot \mathbf{r}) \hat{e},$$

where $E_1(t)$ and $E_2(t)$ are slowly varying complex amplitudes. Suppose that these two beams of light simultaneously illuminate an absorbing material. In cgs units, the intensity in the material will be

$$I(\mathbf{r}, t) = I_1(t) + I_2(t) + \operatorname{Re} 2 \frac{c}{8\pi} (\epsilon/\mu)^{1/2} E_1(t) E_2^*(t) \times \exp(-i\mathbf{k}_{gr} \cdot \mathbf{r}), \quad (3)$$

where $I_1(t)$ and $I_2(t)$ are the individual beam intensities, $\mathbf{k}_{gr} \equiv \mathbf{k}_1 - \mathbf{k}_2$ is the grating k vector, ϵ is the permittivity of the medium, μ is the magnetic permeability, and c is the speed of the light in vacuum.

We will now consider a special case of integrated-intensity gratings: the phase grating resulting from the combination of a nonzero dn/dT , where n is the material refractive index and T is the temperature, and the spatially sinusoidal deposition of heat in an absorbing material. Thus, we require the energy density deposited in the absorbing material in a time interval, τ_p (i.e., the pulse length),

$$W(\mathbf{r}) = \alpha \int_{-\tau_p/2}^{\tau_p/2} I(\mathbf{r}, t) dt, \quad (4)$$

where α is the material absorption coefficient, and we will assume that only a small fraction of the beam intensity is absorbed by the material so that the intensity remains independent of position in directions perpendicular to \mathbf{k}_{gr} . If Φ is the fraction of the deposited energy that becomes heat, then the resulting temperature distribution in the material will be

$$T(\mathbf{r}) = T_0 + \left(\frac{\Phi}{\rho c_v} \right) W(\mathbf{r}), \quad (5)$$

where T_0 is the ambient temperature, ρ is the material density, and c_v is the specific heat at constant volume. We assume that no heat-dissipative effects take place on the time scale, τ_p . Substituting Eqs. (3) and (4) into Eq. (5), we obtain both a uniform increase in the material temperature, ΔT_0 , and a spatially modulated term, ΔT_{gr} ,

$$T(\mathbf{r}) = T_0 + \Delta T_0 + \operatorname{Re} \Delta T_{gr} \exp(-i\mathbf{k}_{gr} \cdot \mathbf{r}), \quad (6)$$

where

$$\Delta T_0 = \frac{\Phi \alpha}{\rho c_v} \int_{-\tau_p/2}^{\tau_p/2} [I_1(t) + I_2(t)] dt \quad (7)$$

and

$$\Delta T_{gr} = \frac{\Phi \alpha}{\rho c_v} 2 \frac{c}{8\pi} (\epsilon/\mu)^{1/2} \int_{-\tau_p/2}^{\tau_p/2} E_1(t) E_2^*(t) dt. \quad (8)$$

The thermal grating arises directly from the spatially modulated term.

Most materials exhibit a temperature-dependent refractive index. Consequently the spatial temperature modulation will become a spatial refractive-index modulation, or phase grating, with amplitude Δn_{gr} :

$$\Delta n_{gr} = \left[\left(\frac{dn}{dT} \right) \frac{\Phi \alpha}{\rho c_v} 2 \frac{c}{8\pi} (\epsilon/\mu)^{1/2} \int_{-\tau_p/2}^{\tau_p/2} E_1(t) E_2^*(t) dt \right], \quad (9)$$

where dn/dT is the derivative of refractive index with respect to temperature, evaluated at $T_0 + \Delta T_0$. The diffraction efficiency, η , of this phase grating will be

$$\eta = K^2 \left| \int_{-\tau_p/2}^{\tau_p/2} E_1(t) E_2^*(t) dt \right|^2, \quad (10)$$

where

$$K = \left(\frac{dn}{dT} \right) \frac{\Phi \alpha}{\rho c_v} 2 \frac{c}{8\pi} (\epsilon/\mu)^{1/2} k_{pr} L. \quad (11)$$

k_{pr} is the probe-beam k vector and L is the sample length.¹² We have assumed the low-diffraction-efficiency limit. If we now explicitly assume *monochromatic* beams, whose field amplitudes, $E_i(t)$, will be constant, Eq. (10) becomes

$$\eta = K^2 |E_1|^2 |E_2|^2 \tau_p^2. \quad (12)$$

Use of Eq. (12) for *relative* numbers yields interesting and useful information.²¹ *Absolute* estimates obtained by using Eq. (12), however, usually give results that are several orders of magnitude larger than experimental values.

Several factors contribute to lowering the efficiency of a thermal grating from this theoretical value. First, the deposition of heat into the sample may require a significant amount of time, so that if relatively short pulses are used and probing occurs simultaneously with or just after excitation, the temperature-modulation buildup will not be complete until after probing occurs. Second, in general, the temperature grating must generate a *density* grating to cause the refractive-index modulation. This process also takes time and will contribute to the observation of a much weaker grating than that predicted by Eq. (12) in short-pulse experiments.²² Third, spatial variations in the excitation-beam intensities can also result in significantly less efficiency than would be expected from a spatially-flat intensity distribution.²³ Finally, temporal variations in the excitation-beam fields in both amplitude and phase will also act to change the efficiency. Of particular importance are temporal variations in the phases of these beams, which can result in a variation of the induced-grating phase and a washing out of the induced grating. These phase variations are similar to those that result in the loss of fringe visibility in the Michelson interferometer.

The inclusion of all the above effects is beyond the scope of this work, and as a result we will not attempt to predict *absolute* diffraction efficiencies but only *relative* efficiencies. We have, however, already included the effects of temporal variations in the excitation-beam fields in Eq. (10), which we will rewrite here as

$$\eta = K^2 \int_{-\tau_p/2}^{\tau_p/2} \int_{-\tau_p/2}^{\tau_p/2} E_1(t_1) E_2^*(t_1) E_1^*(t_2) E_2(t_2) dt_1 dt_2. \quad (13)$$

Rewriting this equation in terms of dimensionless field quantities, $u_i(t)$, we have

$$\eta = K^2 |E_1|^2 |E_2|^2 \int_{-\tau_p/2}^{\tau_p/2} \int_{-\tau_p/2}^{\tau_p/2} u_1(t_1) u_2^*(t_1) u_1^*(t_2) u_2(t_2) dt_1 dt_2, \quad (14)$$

in which $E_i(t) = E_i u_i(t)$, where E_i is a constant field magnitude and $u_i(t)$ contains the time dependence of the excitation-beam fields, i.e., phase and amplitude fluctuations. The expectation value of the modulus of $u_i(t)$ is assumed to be unity.

We will compare results obtained by using Eq. (14) with those of Eq. (12), which is an ideal case involving monochro-

matic radiation (although averaged for a time, τ_p , only). In all comparisons, the several effects mentioned above, which affect the value of K , will cancel when we normalize by the monochromatic-beam diffraction efficiency, $K^2|E_1|^2|E_2|^2\tau_p^2$. So define the normalized thermal-grating diffraction efficiency, $\tilde{\eta}$:

$$\tilde{\eta} = \frac{1}{\tau_p^2} \int_{-\tau_p/2}^{\tau_p/2} \int_{-\tau_p/2}^{\tau_p/2} u_1(t_1)u_2^*(t_1)u_1^*(t_2)u_2(t_2)dt_1dt_2. \quad (15)$$

We must recognize that the thermal-grating diffraction efficiency is a statistical quantity, that is, variations in the diffraction efficiency will occur on a shot-to-shot basis owing to variations in the excitation-beam temporal waveforms. Most experiments measure averages over many shots; it is therefore necessary to consider the ensemble expectation of the normalized diffraction efficiency:

$$\langle \tilde{\eta} \rangle = \left\langle \frac{1}{\tau_p^2} \int_{-\tau_p/2}^{\tau_p/2} \int_{-\tau_p/2}^{\tau_p/2} u_1(t_1)u_2(t_2)u_1^*(t_2)u_2^*(t_1)dt_1dt_2 \right\rangle, \quad (16)$$

where the brackets denote the ensemble expectation operator and we have permuted the factors within the brackets. The time-integration and expectation operators commute, so we have

$$\langle \tilde{\eta} \rangle = \frac{1}{\tau_p^2} \int_{-\tau_p/2}^{\tau_p/2} \int_{-\tau_p/2}^{\tau_p/2} \langle u_1(t_1)u_2(t_2)u_1^*(t_2)u_2^*(t_1) \rangle dt_1dt_2, \quad (17)$$

which is similar to results derived by others.^{6,10,13} The derivation of this result does not depend on the specific properties of the statistics of the radiation field. The product of four fields has arisen because the measured quantity is the square of the fringe intensity-pattern amplitude.

3. THERMAL GRATINGS INDUCED BY PARTIALLY COHERENT LIGHT FROM A SINGLE LASER

Suppose that both excitation beams emanate from the same laser or light source but that one beam traverses a greater distance than the other before reaching the sample material (see Fig. 1). Assume further that the delay between the two beams, τ_d , is much less than the pulse length, τ_p , so that excitation-pulse overlap in time is good. We have, therefore, $u_2(t) = u_1(t + \tau_d)$, so that the integrand in Eq. (17) becomes $\langle u_1(t_1)u_1(t_2 + \tau_d)u_1^*(t_2)u_1^*(t_1 + \tau_d) \rangle$, which is the fourth-order coherence function, $\Gamma^{(4)}(t_1, t_2 + \tau_d; t_2, t_1 + \tau_d)$ for the field $u_1(t)$. Equation (17) now becomes

$$\langle \tilde{\eta} \rangle = \frac{1}{\tau_p^2} \int_{-\tau_p/2}^{\tau_p/2} \int_{-\tau_p/2}^{\tau_p/2} \Gamma^{(4)}(t_1, t_2 + \tau_d; t_2, t_1 + \tau_d) dt_1dt_2. \quad (18)$$

Equation (18) is the ratio of two quantities: the first is the expected efficiency of a thermal grating probed after its formation, when both excitation pulses emanate from the same partially coherent source with relative delay, τ_d , between them, and the second is the diffraction efficiency of a similar grating formed with monochromatic excitation beams. To proceed further, we must assume a statistical model for the partially coherent excitation radiation. It is not sufficient to know merely the frequency spectrum of the excitation radiation, because the recursion relations relating the fourth-order coherence function to second-order coherence functions depend on the radiation model used.

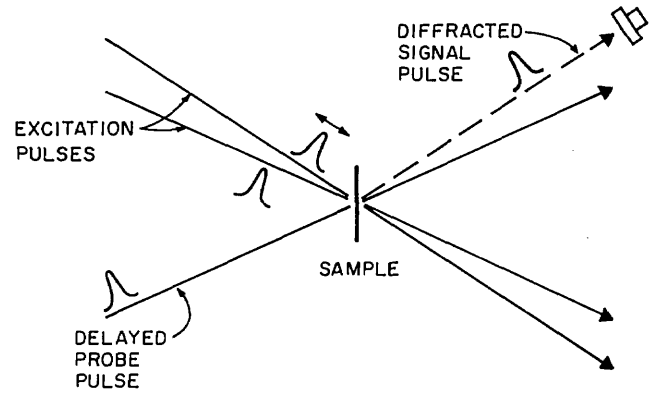


Fig. 1. Experimental arrangement for the study of integrated-intensity gratings. Two excitation pulses experience a variable delay with respect to each other and excite the grating. The probe pulse, further delayed, probes the induced grating, and a detector detects the diffracted beam.

We will use various models for the excitation-beam statistics, including an amplitude-stabilized quasi-monochromatic source²⁴ (which is often used to approximate a single-mode laser) with a Lorentzian frequency spectrum and also a thermal light source¹¹ (which approximates multimode laser sources) with Lorentzian and Gaussian spectra. All these theoretical radiation fields represent ergodic processes, while the pulsed nature of the experiment, which could otherwise destroy ergodicity, is included by integrating for the time τ_p . Later, pulse-shape effects will be included by the inclusion of a deterministic pulse-shape function, $A(t)$, with the random process, $u(t)$, still retaining the convenient property of ergodicity. In general, however, laser light does not represent an ergodic statistical process. And, in particular, the above models do not accurately describe certain types of laser radiation, e.g., mode-locked-laser pulses.¹¹ It should be noted here, though, that each of the above models yields approximately the same quantitative results, which agree well with both intuition and experiment and are therefore adequate for many purposes.

The recursion relation for the fourth-order coherence function of an amplitude-stabilized quasi-monochromatic field is²⁴

$$\Gamma^{(4)}(t_1, t_2, t_3, t_4) = \Gamma^{(2)}(t_1 - t_3)\Gamma^{(2)}(t_2 - t_4) \times \left[\frac{\Gamma^{(2)}(t_1 - t_4)\Gamma^{(2)}(t_2 - t_3)}{\Gamma^{(2)}(t_1 - t_2)\Gamma^{(2)}(t_3 - t_4)} \right], \quad (19)$$

and, for thermal radiation, the recursion relation is¹¹

$$\Gamma^{(4)}(t_1, t_2, t_3, t_4) = \Gamma^{(2)}(t_1 - t_3)\Gamma^{(2)}(t_2 - t_4) + \Gamma^{(2)}(t_1 - t_4)\Gamma^{(2)}(t_2 - t_3). \quad (20)$$

The required integration of these quantities for radiation with Lorentzian and Gaussian line shapes is not difficult, and exact results for various cases are given in Appendix A. The results for all models considered are similar. For the purposes of discussion, we consider thermal radiation with a Lorentzian line shape (a reasonable approximation of a multimode pulsed dye laser). The expected normalized diffraction efficiency to first order in τ_c/τ_p is

$$\langle \tilde{\eta} \rangle \approx \frac{\tau_c}{\tau_p} + \exp(-2|\tau_d/\tau_c|) = \frac{\tau_c}{\tau_p} + |\Gamma^{(2)}(\tau_d)|^2. \quad (21)$$

The exponential (the second-order coherence function) in expression (21) is the well-known "second-order" result,⁷ while the other term corresponds to the background, which results from the incomplete washout of the grating in the finite number of coherence times in the pulse length, despite the relative incoherence of the beams. A few limiting cases are of interest:

(1) When the delay, τ_d , is zero, $\langle \tilde{\eta} \rangle \approx 1$, as expected: when the delay is zero, the relative phase of the two excitation beams does not change, and no grating washout occurs; this situation is equivalent to that of monochromatic excitation beams.

(2) When the pulse length, τ_p , approaches infinity, our result approaches the well-known result for the cw limit: $\langle \tilde{\eta} \rangle = \exp(-2|\tau_d/\tau_c|) = |\Gamma^{(2)}(\tau_d)|^2$. In this case, grating washout will occur for large delays ($\tau_d \gg \tau_c$) but not for small delays ($\tau_d \ll \tau_c$), as expected.

(3) When the coherence time, τ_c , is close to zero, the intensity pattern may exist for a finite time, but its phase dances back and forth extremely fast, again washing out the grating: $\langle \tilde{\eta} \rangle = 0$ for all nonzero values of delay.

(4) The most interesting limit is the case $\tau_d \gg \tau_c$, but with τ_p finite. We then have $\langle \tilde{\eta} \rangle \approx \tau_c/\tau_p$. This means that, despite using a delay much longer than the coherence time, a nonzero expected diffraction efficiency results. This occurs because the finite pulse length allows only τ_p/τ_c coherence times for washout to occur, and, as a result, washout will not be complete. This limit illustrates the primary difference between pulsed and cw experiments, and it shows that thermal gratings can exist in experiments in which excitation beams are drawn from *separate* lasers (equivalent to the $\tau_d \rightarrow \infty$ limit), provided that their average frequencies are equal.

When the delay between pulses approaches the laser pulse length, poor pulse overlap begins to occur and pulse-shape effects must be included in the analysis. When this happens, the τ_c/τ_p -background level will decrease, and when $\tau_d \gg \tau_p$, the background will approach zero because the excitation beams cease to overlap at all. It is easy to see that, if we write the field as $E(t) = EA(t)u(t)$, in which $u(t)$ is the statistical factor that includes the phase of the field and $A(t)$ is a normalized, real, deterministic amplitude function, Eq. (18) becomes

$$\langle \tilde{\eta} \rangle = \frac{1}{\tau_p^2} \int_{-\infty}^{\infty} \int_{-\infty}^{\infty} A(t_1)A(t_2 + \tau_d)A(t_1 + \tau_d)A(t_2) \times \Gamma^{(4)}(t_1, t_2 + \tau_d; t_1 + \tau_d, t_2) dt_1 dt_2. \quad (22)$$

This expression is also easily evaluated for the various radiation models of interest, and Appendix B contains exact expressions for thermal radiation with Gaussian and hyperbolic-secant-squared pulse shapes. We can, however, derive a simple and intuitive expression, analogous to relation (21), when $\tau_c \ll \tau_p$. If we assume thermal radiation, we obtain

$$\langle \tilde{\eta} \rangle \approx \frac{\tau_c}{\tau_p} \int_{-\infty}^{\infty} I(t)I(t + \tau_d)dt + |\Gamma^{(2)}(\tau_d)|^2, \quad (23)$$

independent of the precise shapes of the pulse and line and where $I(t)$ is the normalized intensity: $I(t) \equiv A^2(t)$ defined

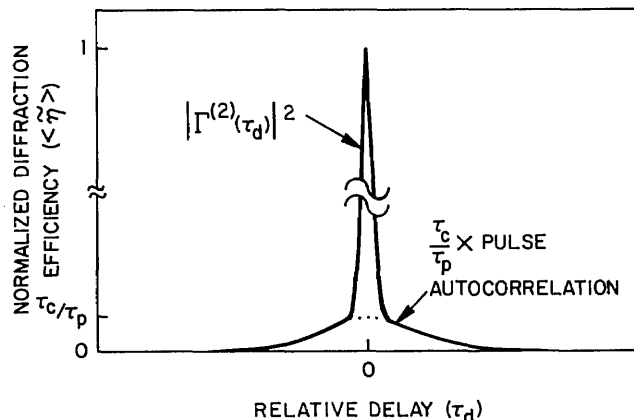


Fig. 2. Plot of theoretical diffraction efficiency versus delay between excitation beams for the case of $\tau_c \ll \tau_p$.

so that when $\tau_d = 0$, the integral in expression (23) is unity. As before, the second term is the well-known second-order result,⁷ and the first term is the background, now seen to be the pulse autocorrelation function. The magnitude of the first term is still τ_c/τ_p smaller than the second, but now only when $\tau_d = 0$; when $|\tau_d|$ increases to values on the order of τ_p , the first term's strength decreases (see Fig. 2).

4. COMPARISON WITH EXPERIMENT

These expressions describe a grating experiment performed by Eichler *et al.*,⁷ in which picosecond pulses from a frequency-doubled Nd:YAG laser were split and interfered to form an integrated-intensity grating (probably thermal but possibly having a long-lived population component, also) in a solution of Rhodamine 6G dissolved in ethanol. Eichler *et al.* fitted their data to a second-order theory, and their best fit is shown as the dashed line in Fig. 3. We have fitted their data to a fourth-order theory, shown by the solid line, resulting from a hyperbolic-secant-squared pulse shape and thermal Lorentzian line and using expression (23):

$$\langle \tilde{\eta} \rangle \approx \frac{\zeta \tau_c}{\tau_p} \left[\frac{\zeta \tau_d / \tau_p \cosh(\zeta \tau_d / \tau_p) - \sinh(\zeta \tau_d / \tau_p)}{\sinh^3(\zeta \tau_d / \tau_p)} \right] + \exp(-2|\tau_d/\tau_d|), \quad (24)$$

where $\zeta = 1.7627$. The fourth-order theory yields a much better fit. We derive the pulse length from the width of the "background" to be 26.5 ± 0.5 psec, a bit higher than the value measured by Eichler *et al.* with a streak camera: 22 ± 4 psec. The smaller error bars accompanying our value reflect the multishot averaging in the grating experiment (compared to the single-shot nature of the streak camera measurement). We also derive a coherence time, τ_c , of 8.5 ± 0.5 psec from the width of the central spike, also larger than the experimental value measured by Eichler *et al.* of 2.7 psec, and obtained from the expression $\tau_c = 1/\pi\delta\nu$, where $\delta\nu = 1.2 \times 10^{11}$ Hz. This discrepancy is probably due to the fact that Eichler *et al.* measured $\delta\nu$ by using different pump powers and alignments than were used in this experiment. Significantly, the theory fits the data reasonably well, despite the fact that the ratio of the magnitudes of the two terms is determined by these two times and cannot be independently curve fitted.

It should be noted that, in using expression (23), we have

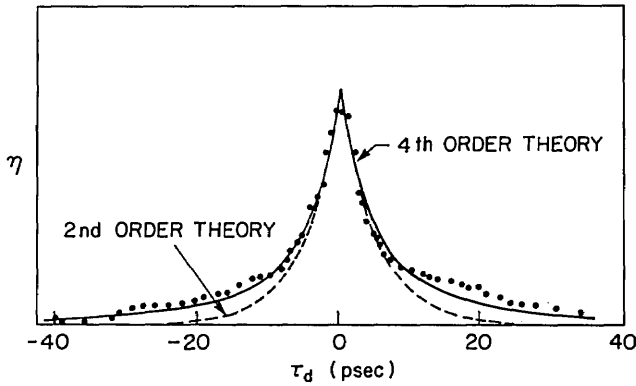


Fig. 3. Experimental integrated-intensity-grating diffraction efficiency versus relative delay in an experiment of Eichler *et al.*⁷ The dashed curve represents the best fit to a (cw-limit) second-order theory, while the solid curve represents the best fit to an approximation to the fourth-order theory developed here. Note that the fourth-order theory yields a much better fit in the wings of the data, where only incomplete washout of the grating occurs, and poor pulse-overlap limits the diffraction efficiency.

employed a theory that assumes that $\tau_c \ll \tau_p$ to fit data in which these quantities apparently differ by only a factor of approximately 3. The error introduced by this assumption will be of the order of τ_c^2/τ_p^2 , and, in general, the coefficient multiplying this quantity is less than unity (see Appendix B). The maximum error anticipated here is a few percent. Significantly, the use of exact results for radiation with a less appropriate (Gaussian) pulse shape [Eq. (B5)] fit the data equally well. The error introduced by the use of a thermal-radiation model to describe the mode-locked pulses is probably larger.

5. PULSE-LENGTH MEASUREMENT USING THERMAL GRATINGS

Eichler *et al.* performed their experiment to demonstrate that integrated-intensity gratings can be used to measure radiation coherence times. We have observed that their experiment also provides an autocorrelation measurement for the pulse length. Because thermal gratings can be quite efficient and because automatically phase-matched geometries (such as the polarization spectroscopy geometry used by Song *et al.*²⁵ and some background-free geometries employing counterpropagating excitation and probe beams²⁶) exist for the performance of thermal-grating experiments, such a technique may be preferred over current techniques, such as second-harmonic generation (SHG).

We can compare this thermal-grating pulse-autocorrelation method with SHG methods by noting that the expected normalized SHG energy efficiency $\langle \tilde{\eta}_{\text{SHG}} \rangle$ can be written as

$$\langle \tilde{\eta}_{\text{SHG}} \rangle = \int_{-\infty}^{\infty} \langle |A(t)A(t + \tau_d)u(t)u(t + \tau_d)|^2 \rangle dt, \quad (25)$$

where as before $A(t)$ represents a smooth deterministic pulse-shape envelope and $u(t)$ contains the phase and amplitude fluctuations. Rewriting this expression, we have

$$\langle \tilde{\eta}_{\text{SHG}} \rangle = \int_{-\infty}^{\infty} A^2(t)A^2(t + \tau_d)\Gamma^{(4)}(t, t + \tau_d; t, t + \tau_d)dt. \quad (26)$$

This expression is analogous to Eq. (22), which gives the

normalized thermal-grating diffraction efficiency if probing occurs after its formation.

We would like to simplify these expressions further. Observing that, for Fourier-transform-limited pulses, $\tau_c \approx \tau_p$, and partial-coherence effects will be absent (both methods yield the pulse autocorrelation without central spikes). Thus we must consider the $\tau_c \ll \tau_p$ regime. To do so, a radiation model must be chosen. We will again choose a thermal model, for simplicity but also because, when $\tau_c \ll \tau_p$, good mode locking has evidently not occurred and considerable randomness in the modes' phases must exist. Copying the result for thermal gratings, expression (23), and using the recursion relation for $\Gamma^{(4)}$, Eq. (20), we obtain

$$\langle \tilde{\eta}_{\text{TG}} \rangle \approx \frac{\tau_c}{\tau_p} \int_{-\infty}^{\infty} I(t)I(t + \tau_d)dt + |\Gamma^{(2)}(\tau_d)|^2 \quad (27)$$

and

$$\langle \tilde{\eta}_{\text{SHG}} \rangle \approx \int_{-\infty}^{\infty} I(t)I(t + \tau_d)dt + |\Gamma^{(2)}(\tau_d)|^2, \quad (28)$$

when $\tau_c \ll \tau_p$; TG stands for thermal grating. Thus the autocorrelation function is weaker in thermal-grating methods by a factor of τ_c/τ_p . For pulses that are far from Fourier-transform limited, the autocorrelation may be difficult to see next to the central spike. That this background attenuation occurs is no surprise: thermal-grating methods are sensitive to phase variations in the beams, and the resultant fringe washout reduces diffraction efficiency. It must also be admitted that sensitivity to *phase* is in general not desirable in a pulse-*amplitude* measurement technique. Thus SHG or other methods, such as two-photon fluorescence, that measure only the pulse amplitude yield more desirable information, while thermal-grating methods are less expensive and are easier to perform.

On the other hand, because of the reduced autocorrelation background due to this phase sensitivity, thermal-grating techniques may provide an excellent measure of radiation coherence times, as suggested by Eichler *et al.* It must be remembered, however, that one measures a fourth-order coherence function, not a second-order coherence function, and unless the experimenter knows the appropriate model, i.e., recursion relation, for his radiation, it may not be possible to extract $\Gamma^{(2)}(t)$ from the measurement.

6. INCLUSION OF GRATING-RELAXATION EFFECTS

If the grating decay time is of the order of the laser pulse length, a new theory incorporating this decay, the laser pulse shape, and perhaps partial coherence effects must be developed. This is easily done,^{10,12} and Eq. (17) becomes

$$\begin{aligned} \langle \tilde{\eta}(t) \rangle = & \int_{-\infty}^t \int_{-\infty}^t A(t_1)A(t_2 + \tau_d)A(t_2)A(t_1 + \tau_d) \\ & \times \Gamma^{(4)}(t_1, t_2 + \tau_d; t_2, t_1 + \tau_d)h(t - t_1)h(t - t_2)dt_1dt_2, \end{aligned} \quad (29)$$

where $h(t)$ is the grating decay function. The diffraction efficiency is now necessarily time dependent because, using pulses, the grating will eventually decay away completely. Usually the grating decay function will be exponential: $h(t)$

$= \exp(-t/\tau_{th})\theta(t)$, where τ_{th} is the decay time scale and $\theta(t)$ is the unit step function. We assume thermal radiation and again work in the regime $\tau_c \ll \tau_p$. Also, we assume square pulses, $A(t) = \text{rect}(t/\tau_p)$, for simplicity, and calculate the diffraction efficiency for points in time after the two pulses have passed through the sample material. For delays that yield at least some pulse overlap,

$$\langle \tilde{\eta}(t) \rangle = \exp\left(-\frac{2t + \tau_d}{\tau_{th}}\right) \left[\tau_c \tau_{th} \sinh\left(\frac{\tau_p - |\tau_d|}{\tau_{th}}\right) + 4\tau_{th}^2 |\Gamma^{(2)}(\tau_d)|^2 \sinh^2\left(\frac{\tau_p - |\tau_d|}{2\tau_{th}}\right) \right] \quad (30)$$

We can more easily compare Eq. (30) with previous results if we renormalize so that the coefficient of $|\Gamma^{(2)}(\tau_d)|^2$ is one and also assume that $|\tau_d| \ll \tau_p$:

$$\langle \tilde{\eta}(t) \rangle \propto \frac{\tau_c}{4\tau_{th}} \frac{\sinh(\tau_p/\tau_{th})}{\sinh^2(\tau_p/2\tau_{th})} + |\Gamma^{(2)}(\tau_d)|^2 \quad (31)$$

Expression (31) simplifies significantly in a few limiting cases:

(1) $\tau_{th} \ll \tau_p$:

$$\langle \tilde{\eta}(t) \rangle \propto \frac{\tau_c}{2\tau_{th}} + |\Gamma^{(2)}(\tau_d)|^2 \quad (32)$$

Thus, within a factor of 2, the thermal-grating decay time replaces the pulse length in expression (21). This makes sense because, recalling the argument leading to expressions (1) and (2), deposited energy now remains for a time, τ_{th} , only. As a result, we must now consider the number of coherence times in a thermal-grating decay time rather than in a pulse length, because grating-fringe contributions created more than τ_{th} ago are no longer present.

(2) $\tau_p \ll \tau_{th}$:

$$\langle \tilde{\eta}(t) \rangle \propto \frac{\tau_c}{\tau_p} + |\Gamma^{(2)}(\tau_d)|^2 \quad (33)$$

This result is just expression (21), as expected.

(3) $\tau_p < \tau_{th}$:

$$\langle \tilde{\eta}(t) \rangle \propto \frac{\tau_c}{\tau_p} \left[1 + \frac{1}{12} \left(\frac{\tau_p}{\tau_{th}} \right)^2 \right] + |\Gamma^{(2)}(\tau_d)|^2 \quad (34)$$

From this approximate result, we can see that the thermal-grating decay time must be as short as, or shorter than, the pulse length before decay effects are observed. The overall strength of the diffraction process depends sensitively on the thermal-grating decay time, but the ratio of the two terms, as indicated in expression (34), does not *sensitively* depend on τ_p/τ_{th} unless τ_{th} is less than τ_p .

7. INTEGRATED-INTENSITY GRATINGS INDUCED BY PARTIALLY COHERENT LIGHT FROM TWO SEPARATE LASERS

In the limit of large delays (specifically, $\tau_c \ll \tau_d$), the problem approximates that of using two separate, independent sources of the same frequency. We now specifically consider the problem of integrated-intensity-grating formation with two independent sources with potentially different frequencies. This problem is of interest because many researchers employing (two-excitation-laser) variable-fre-

quency, induced-grating techniques to measure excited-state relaxation times have instead seen only thermal-grating effects.^{9,12} An understanding of thermal gratings in two-excitation-laser experiments is important for the development of techniques for their suppression.²⁷

The simple argument at the beginning of Section 2 shows why a nonzero diffraction efficiency is to be expected when the frequency difference between the two excitation lasers, $\Delta\omega$, is zero. We now generalize and formalize that result for all values of $\Delta\omega$. Recalling Eq. (17) and observing that the two radiation fields, $u_1(t)$ and $u_2(t)$, will now be independent, we can separate the expectation operator into the product of two expectations. The expected normalized diffraction efficiency will now be

$$\langle \tilde{\eta}(\Delta\omega) \rangle = \frac{1}{\tau_p^2} \int_{-\tau_p/2}^{\tau_p/2} \int_{-\tau_p/2}^{\tau_p/2} \Gamma_1^{(2)}(t_1; t_2) \Gamma_2^{(2)*}(t_1; t_2) dt_1 dt_2, \quad (35)$$

where $\Gamma_i^{(2)}(t_j; t_k)$ is the second-order statistical coherence function of the i th excitation-beam radiation field.

Because the excitation lasers will, in general, lase at different frequencies, $\Gamma_1^{(2)}(t_1; t_2) \neq \Gamma_2^{(2)}(t_1; t_2)$, even if the lasers are otherwise identical. For wide-sense-stationary light sources, the arguments of the coherence functions can be written: $t_1 - t_2$. As a result,

$$\langle \tilde{\eta}(\Delta\omega) \rangle = \frac{1}{\tau_p^2} \int_{-\tau_p/2}^{\tau_p/2} \int_{-\tau_p/2}^{\tau_p/2} \Gamma_1^{(2)}(t_1 - t_2) \times |\Gamma_2^{(2)*}(t_1 - t_2)| dt_1 dt_2, \quad (36)$$

A routine change of variables ($t = t_1 - t_2$; $s = t_1 + t_2$) allows one integration to be performed trivially:

$$\langle \tilde{\eta}(\Delta\omega) \rangle = \frac{1}{2\tau_p'} \int_{-\tau_p'}^{\tau_p'} (1 - |t/\tau_p'|) |\Gamma_1^{(2)}(t) \Gamma_2^{(2)*}(t)| dt, \quad (37)$$

where $\tau_p' = \tau_p/\sqrt{2}$. Equation (37) can be evaluated exactly for the various statistical models we have been considering.

A general result can be obtained, however, in a useful limiting case. When each coherence time is much less than the pulse length, the functions $|\Gamma_i^{(2)}(t)|^2$ will be close to zero for all values of t for which the factor $(1 - |t/\tau_p|)$ deviates significantly from unity. This factor can thus be set equal to one with good accuracy. In addition, the integration limits may be extended to $-\infty$ and $+\infty$, respectively, in this limit. We then have, if $\tau_c \ll \tau_p$:

$$\langle \tilde{\eta}(\Delta\omega) \rangle \approx \frac{1}{\tau_p} \int_{-\infty}^{\infty} \Gamma_1^{(2)}(t) \Gamma_2^{(2)*}(t) dt, \quad (38)$$

and thus the thermal-grating line shape is just the Fourier transform of the product of the magnitudes of the second-order coherence functions of the excitation fields. Expression (38) can be rewritten in a different form using the Wiener-Khinchine theorem,¹¹ assuming wide-sense-stationary excitation fields:

$$\langle \tilde{\eta}(\Delta\omega) \rangle \approx \frac{1}{\tau_p} \int_{-\infty}^{\infty} I_1(\omega) I_2(\omega) d\omega, \quad (39)$$

which is just the convolution of the excitation frequency spectra: If we substitute into expression (38) or (39) the appropriate functions corresponding to Lorentzian and Gaussian line shapes, we obtain thermal-grating line shapes

that are similar but are wider by factors of 2 and $\sqrt{2}$, respectively. Also, as expected, the maximum value of $\langle \tilde{\eta}(\Delta\omega) \rangle$, occurring at $\Delta\omega = 0$, is τ_c/τ_p in both cases.

8. COMPARISON WITH EXPERIMENT

We performed a two-excitation-laser, variable-frequency induced-grating experiment with the sample material malachite green dissolved in ethanol (3×10^{-4} mol/liter) and simultaneously measured both the laser line shapes and the thermal-grating line shape. Our experimental apparatus is shown in Fig. 4. Three Q-switched Nd:YAG laser-pumped pulsed dye lasers provided $\sim 300\text{-}\mu\text{J}$ pulses of $\sim 7\text{-nsec}$ duration at a repetition rate of 10 pulses/sec. Two dye lasers provided excitation beams (at 615 nm), while the third (at 610 nm) provided the probe beam. Probing occurred simultaneously with the grating formation. The two excitation lasers were adjusted to have equal linewidths (0.8-cm^{-1} FWHM), and their line shapes were observed to be similar. The laser linewidths were monitored with a 1-mm-thick fused silica étalon (3.3-cm^{-1} free-spectral range and a finesse of 30), and the lasers were adjusted until they had the same linewidth. The precise line shape of the variable-frequency excitation laser was obtained by detecting the transmission of this beam through the above étalon during the experi-

ment. The thermal-grating diffraction efficiency and étalon transmission were measured simultaneously. Figure 5 shows an example of these measurements. Only one laser line shape is shown. The laser line shape is intermediate between Gaussian and Lorentzian. We therefore expect the ratio of the thermal-grating linewidth and laser linewidth to be between $\sqrt{2}$ and 2. The measured value is 1.9 ± 0.2 (corrected slightly for the étalon linewidth), within the above theoretical range. The thermal-grating and laser line shapes are also similar. Finally, it should also be mentioned that a second-order theory predicts no thermal-grating diffraction at all in this experiment.

9. CONCLUSIONS

We studied the theory of the formation of integrated-intensity gratings with partially coherent pulsed-light sources. Evaluating the theory for several radiation models yielded simple expressions for the thermal-grating diffraction efficiency, containing only two terms in the limit $\tau_c \ll \tau_p$, a coherence term and a pulse-autocorrelation term, assuming a thermal model for the excitation radiation.

Applying this theory to a previously performed experiment, we obtained better agreement with the experimental data. We discussed thermal-grating techniques for pulse-length and coherence time measurement, and included grating-decay effects in the model. Finally we considered the case of integrated-intensity-grating formation with beams from two separate and independent sources of arbitrary frequencies. Performing an experiment using three separate lasers, we found this theory and the experiment to be in agreement.

APPENDIX A: EXPRESSIONS FOR SEVERAL RADIATION MODELS

The amplitude-stabilized quasi-monochromatic radiation field is described by the expression

$$E(t) = A_0 \exp(i\omega_0 t + \phi(t) + \Phi_0),$$

where A_0 is a constant field amplitude, Φ_0 is a random variable uniformly distributed over the interval $[-\pi, \pi]$, and $\phi(t)$ is a random process. Picinbono and Boileau²⁴ describe this type of light in more detail. Thermal radiation fields correspond to the sum of a large number of such sources and are described in more detail in the text of Goodman,¹¹ whose conventions we will follow.

Gaussian and Lorentzian frequency spectra, $I_G(\omega)$ and $I_L(\omega)$, will be assumed to be of the forms

$$I_G(\omega) = \frac{4\sqrt{\pi \ln 2}}{\delta\omega} \exp\left[-4 \ln 2 \left(\frac{\omega - \omega_0}{\delta\omega}\right)^2\right] \quad (A1)$$

and

$$I_L(\omega) = \frac{4/\delta\omega}{1 + 4\left(\frac{\omega - \omega_0}{\delta\omega}\right)^2}, \quad (A2)$$

where $\delta\omega$ is the FWHM of each frequency spectrum. We will use the following expressions for the second-order coherence functions:

$$\Gamma^{(2)}(t) = \exp(i\omega_0 t) \exp(-|t/\tau_c|) \quad (A3)$$

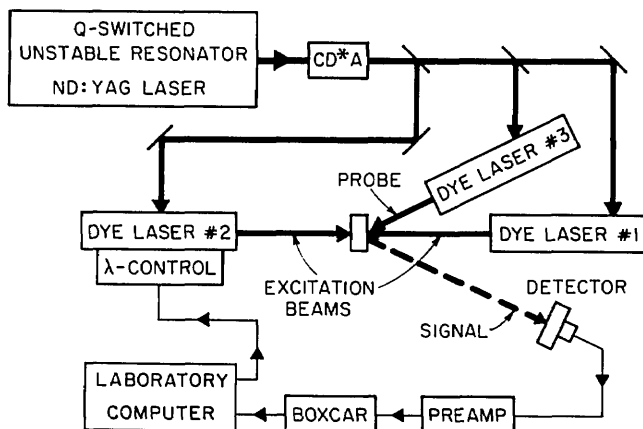


Fig. 4. Experimental apparatus for the study of integrated-intensity gratings formed with two independent excitation sources.

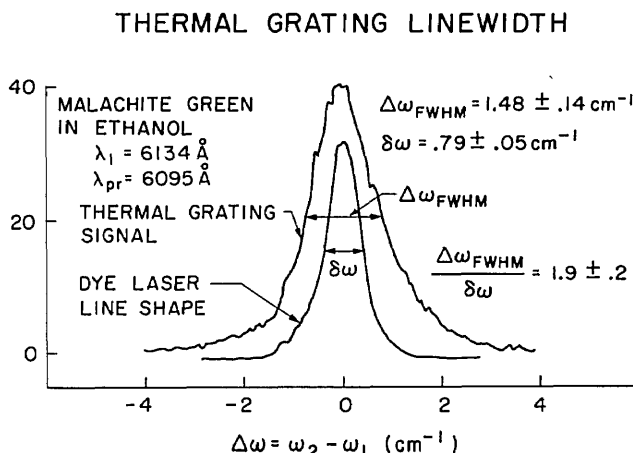


Fig. 5. Two-excitation-laser integrated-intensity-grating diffraction efficiency versus $\Delta\omega$. Also shown is a dye-laser line shape.

for a Lorentzian line, in which $\tau_c = 2/\delta\omega$, and

$$\Gamma^{(2)}(t) = \exp(i\omega_0 t) \exp(-\pi t^2/2\tau_c^2) \quad (\text{A4})$$

for a Gaussian line, in which $\tau_c = \sqrt{8\pi \ln 2}/\delta\omega$. In each of the above expressions, τ_c is the radiation-field coherence time, which is necessarily less than the pulse length, τ_p , and which is defined so that

$$\tau_c = \int_{-\infty}^{\infty} |\Gamma^{(2)}(t)|^2 dt. \quad (\text{A5})$$

The diffraction-efficiency relations can be evaluated without the need for further approximations. We obtain, for an amplitude-stabilized quasi-monochromatic Lorentzian line,

$$\langle \tilde{\eta} \rangle = \left[\frac{\tau_c}{\tau_p} - \frac{1}{2} \frac{\tau_c^2}{\tau_p^2} \right] + \left[1 - 2 \frac{\tau_d}{\tau_p} + \frac{\tau_d^2}{\tau_p^2} + \frac{\tau_d \tau_c}{\tau_p^2} + \frac{1}{2} \frac{\tau_c^2}{\tau_p^2} - \frac{\tau_c}{\tau_p} \right] \exp(-2|\tau_d/\tau_c|), \quad (\text{A6})$$

which, to first order in τ_c/τ_p and τ_d/τ_p , is

$$\langle \tilde{\eta} \rangle \approx \frac{\tau_c}{\tau_p} + \left[1 - 2 \frac{\tau_d}{\tau_p} - \frac{\tau_c}{\tau_p} \right] \exp(-2|\tau_d/\tau_c|). \quad (\text{A7})$$

Other statistical models give similar results. For a thermal Lorentzian line, we obtain

$$\langle \tilde{\eta} \rangle = \left[\frac{\tau_c}{\tau_p} - \frac{1}{2} \frac{\tau_c^2}{\tau_p^2} \right] + \left[1 + \frac{\tau_c^2}{\tau_p^2} \right] \exp(-2|\tau_d/\tau_c|), \quad (\text{A8})$$

which, to first order in τ_c/τ_p , is

$$\langle \tilde{\eta} \rangle \approx \frac{\tau_c}{\tau_p} + \exp(-2|\tau_d/\tau_c|) \quad (\text{A9})$$

and which, in general, looks much like Eq. (A6). And for a thermal Gaussian line, we find

$$\langle \tilde{\eta} \rangle = \sqrt{2} \frac{\tau_c}{\tau_p} \operatorname{erf} \left(\sqrt{2} \frac{\tau_p}{\tau_c} \right) + \exp(-\pi \tau_d^2/\tau_c^2) - \frac{1}{\pi} \frac{\tau_c^2}{\tau_p^2} [1 - \exp(-\pi \tau_p^2/\tau_c^2)], \quad (\text{A10})$$

which, to first order in τ_c/τ_p , becomes

$$\langle \tilde{\eta} \rangle \approx \sqrt{2} \frac{\tau_c}{\tau_p} + \exp(-\pi \tau_d^2/\tau_c^2), \quad (\text{A11})$$

which also looks similar to the other curves. The Gaussian shape deviates, of course, from the simple exponentials obtained for the Lorentzian lines, but the limiting cases are as expected, with the $\sqrt{2}$ having its origins in the definitions of τ_c and τ_p .

APPENDIX B: THE INCLUSION OF PULSE-SHAPE EFFECTS

We will assume a Gaussian pulse shape:

$$A(t) = \left(\frac{4 \ln 2}{\pi \tau_p} \right)^{1/4} \exp[-2 \ln 2 (t^2/\tau_p^2)], \quad (\text{B1})$$

where τ_p is the FWHM of the intensity. $A(t)$ is normalized so that

$$\int_{-\infty}^{\infty} A^4(t) dt = \int_{-\infty}^{\infty} I^2(t) dt = 1, \quad (\text{B2})$$

i.e., a dimensionless, unity-magnitude autocorrelation.

For a thermal Lorentzian line and a Gaussian pulse shape then, Eq. (22) becomes

$$\langle \tilde{\eta} \rangle = \exp[-2 \ln 2 (\tau_d^2/\tau_p^2)] \left\{ \exp \left(\frac{\tau_p^2/\tau_c^2}{2 \ln 2} \right) \times \left[1 - \operatorname{erf} \left(\frac{\tau_p/\tau_c}{\sqrt{2 \ln 2}} \right) \right] + \exp(-2|\tau_d/\tau_c|) \right\}. \quad (\text{B3})$$

When $\tau_c \ll \tau_p$, this result simplifies considerably:

$$\langle \tilde{\eta} \rangle \approx \sqrt{\frac{2 \ln 2}{\pi}} \left(\frac{\tau_c}{\tau_p} \right) \exp[-2 \ln 2 (\tau_d^2/\tau_p^2)] + \exp(-2|\tau_d/\tau_c|). \quad (\text{B4})$$

A thermal Gaussian line with a Gaussian pulse shape yields

$$\langle \tilde{\eta} \rangle = \exp[-2 \ln 2 (\tau_d^2/\tau_p^2)] \left\{ \sqrt{\frac{2 \ln 2}{\pi}} \left(\frac{\tau_c}{\tau_p} \right) \times \left(1 + \frac{2 \ln 2}{\pi} \frac{\tau_c^2}{\tau_p^2} \right)^{-1/2} + \exp(-\pi \tau_d^2/\tau_c^2) \right\}, \quad (\text{B5})$$

which also simplifies when $\tau_c \ll \tau_p$:

$$\langle \tilde{\eta} \rangle \approx \sqrt{\frac{2 \ln 2}{\pi}} \left(\frac{\tau_c}{\tau_p} \right) \exp[-2 \ln 2 (\tau_d^2/\tau_p^2)] + \exp(-\pi \tau_d^2/\tau_c^2). \quad (\text{B6})$$

The fourth-order theory for a thermal Lorentzian line using a hyperbolic-secant-squared pulse shape results in a diffraction efficiency:

$$\langle \tilde{\eta} \rangle \approx \frac{\zeta \tau_c}{\tau_p} \left[\frac{\zeta \tau_d/\tau_p \cosh(\zeta \tau_d/\tau_p) - \sinh(\zeta \tau_d/\tau_p)}{\sinh^3(\zeta \tau_d/\tau_p)} \right] + \exp(-2|\tau_d/\tau_c|), \quad (\text{B7})$$

where $\zeta = 1.7627$.

ACKNOWLEDGMENTS

R. Trebino would like to acknowledge the helpful conversations with and advice of J. W. Goodman. The authors are grateful for financial assistance from the U.S. Air Force Office of Scientific Research.

REFERENCES AND NOTES

1. G. Martin and R. W. Hellwarth, "Infrared-to-optical image conversion by Bragg reflection from thermally induced index changes," *Appl. Phys. Lett.* **34**, 371-373 (1979).
2. R. K. Jain and M. B. Klein, "Degenerate four-wave mixing in semiconductors," in *Optical Phase Conjugation*, R. A. Fisher, ed. (Academic, New York, 1983), pp. 365-366.
3. J. R. Salcedo, A. E. Siegman, D. D. Dlott, and M. D. Fayer, "Dynamics of energy transport in molecular crystals: the picosecond transient grating method," *Phys. Rev. Lett.* **41**, 131-134 (1978).
4. K. A. Nelson, D. R. Lutz, M. D. Fayer, and L. Madison, "Laser-induced phonon spectroscopy, optical generation of ultrasonic

- waves and investigation of electronic excited-state interactions in solids," *Phys. Rev. B* **24**, 3261-3275, (1981).
5. J. R. Salcedo and A. E. Siegman, "Laser induced photoacoustic grating effects in molecular crystals," *IEEE J. Quant. Electron.* **QE-15**, 250-256 (1979).
 6. V. S. Idiatulin and Yu. N. Teryaev, "Transient gratings in a nonlinear medium," *Opt. Quantum Electron.* **14**, 51-56 (1982).
 7. H. J. Eichler, U. Klein, and D. Langhans, "Coherence time measurement of picosecond pulses by a light-induced grating method," *Appl. Phys.* **21**, 215-219 (1980).
 8. R. Baltrameyunas, Yu. Vaitkus, R. Dannelyus, M. Pytrauskas, and A. Piskarskas, "Applications of dynamic holography in determination of coherence times of single picosecond light pulses," *Sov. J. Quantum Electron.* **12**, 1252-1254 (1982).
 9. J. R. Andrews and R. M. Hochstrasser, "Transient grating studies of energy deposition in radiationless processes," *Chem. Phys. Lett.* **76**, 207-212, (1980).
 10. Z. Vardeny and J. Tauc, "Picosecond coherence coupling in the pump and probe technique," *Opt. Commun.* **39**, 396-400 (1981).
 11. J. W. Goodman, *Statistical Optics* (Wiley, New York, 1985).
 12. R. Trebino, "Subpicosecond-relaxation studies using tunable-laser-induced-grating techniques," Ph.D. dissertation (Stanford University, Stanford, Calif., 1983).
 13. B. S. Wherrett, A. L. Smirl, and T. F. Boggess, "Theory of degenerate four-wave mixing in picosecond excitation-probe experiments," *IEEE J. Quantum Electron.* **QE-19**, 680-689 (1983).
 14. C. V. Shank and D. H. Auston, "Parametric coupling in an optically excited plasma in Ge," *Phys. Rev. Lett.* **34**, 479 (1975).
 15. A. von Jena and H. E. Lessing, "Coherent coupling effects in picosecond absorption experiments," *Appl. Phys.* **19**, 131-144 (1979).
 16. T. F. Heinz, S. L. Palfrey, and K. B. Eisenthal, "Coherent coupling effects in pump-probe measurements with collinear, copropagating beams," *Opt. Lett.* **9**, 359-361 (1984).
 17. W. M. Grossman and D. M. Shemwell, "Coherence lengths and phase conjugation by degenerate four-wave mixing," *J. Appl. Phys.* **51**, 914-916. (1980).
 18. M. Schubert, K.-E. Süsse, and W. Vogel, "Influence of chaotic pump radiation with finite bandwidth on the intensity correlation of resonance fluorescence radiation," *Opt. Commun.* **30**, 275-278 (1979).
 19. H. J. Kimble and L. Mandel, "Resonance fluorescence with excitation of finite bandwidth," *Phys. Rev. A* **15**, 689-699 (1977).
 20. It appears, from our discussion, that in the cw limit the diffraction efficiencies in both cases go to infinity. This is, of course, not the case because material relaxation prevents the buildup of infinite grating strength. When the pulse is longer than the material relaxation time, the relaxation time then replaces the pulse length in the above argument. Section 6 treats this effect in greater detail. In any event, the argument presented in the text is intended to give relative grating strengths only.
 21. Equations (11) and (12) explain why thermal gratings have obscured population gratings in grating experiments on dyes dissolved in ethanol but not in experiments using water as a solvent. The solvent-dependent factors in Eq. (11) result in a thermal-grating diffraction efficiency proportional to $[(dn/dT)/\rho c_v]^2$, with other factors depending on the solute, laser light, or beam geometry or exhibiting little variation.⁹ The value of $[(dn/dT)/\rho c_v]^2$ for ethanol is more than 100 times that for water.
 22. R. C. Desai, M. D. Levenson, and J. A. Baker, "Forced Rayleigh scattering: thermal and acoustic effects in phase-conjugate wave-front generation," *Phys. Rev. A* **27**, 1968-1976 (1983).
 23. A. E. Siegman, "Bragg diffraction of a Gaussian beam by a crossed-Gaussian volume grating," *J. Opt. Soc. Am.* **67**, 545-550 (1955).
 24. B. Picinbono and E. Boileau, "Higher-order coherence functions of optical fields and phase fluctuations," *J. Opt. Soc. Am.* **58**, 784-789 (1968).
 25. J. J. Song, J. H. Lee, and M. D. Levenson, "Picosecond relaxation measurements by polarization spectroscopy in condensed phases," *Phys. Rev. A* **17**, 1439-1447 (1978).
 26. J. R. Salcedo, A. E. Siegman, D. D. Dlott, and M. D. Fayer, "Dynamics of energy transport in molecular crystals: the picosecond transient grating method," *Phys. Rev. Lett.* **41**, 131-134 (1978).
 27. R. Trebino, A. E. Siegman, and C. L. Ladera, "Suppression of thermal gratings in polarization spectroscopy," *J. Opt. Soc. Am. B* **1**, 549-550 (1984).